Modeling and analysis of LOFAR scintillation data

M. Grzesiak, Mariusz Pożoga, Barbara Matyjasiak, Dorota Przepiórka,
Hanna Rothkaehl, Katarzyna Budzińska, and Barbara Atamaniuk

EGU General Assembly 2021, online, 19–30 Apr 2021,
EGU21-6582, https://doi.org/10.5194/egusphere-egu21-6582, 2021.

Modeling and analysis of LOFAR scintillation data

Scintillation - fluctuations of wave characteristics after passing through medium with variable refractive index

Interferometry in low frequencies (10-240 MHz)

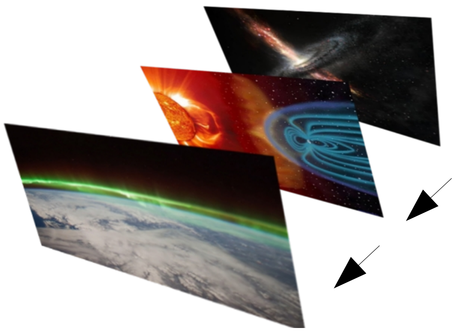

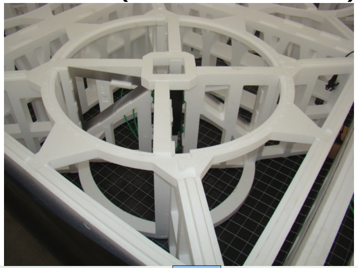

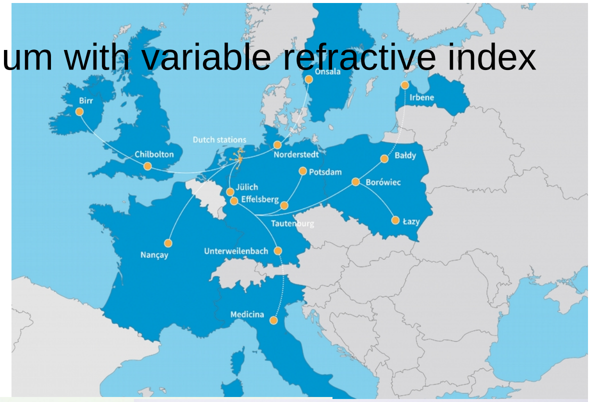

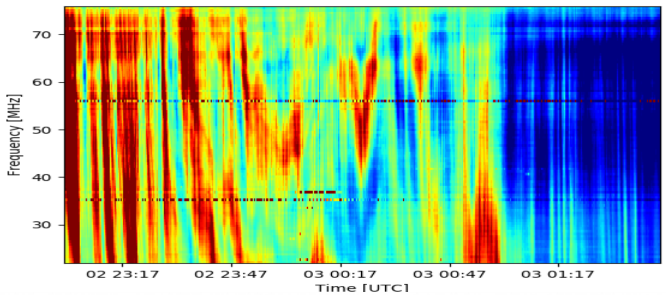

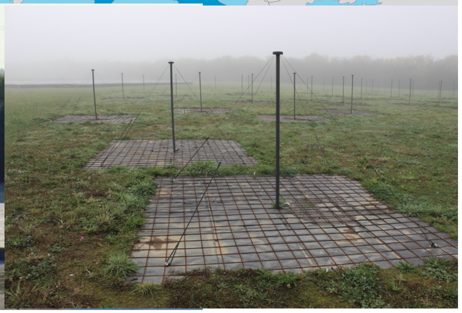

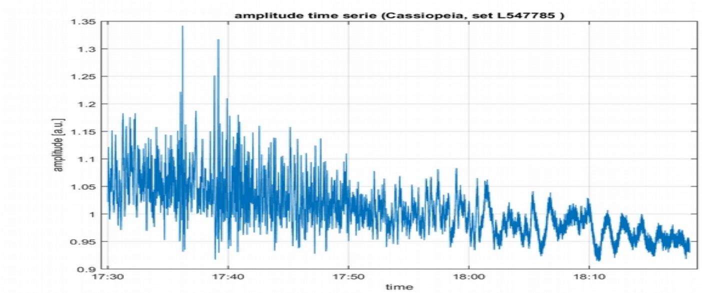

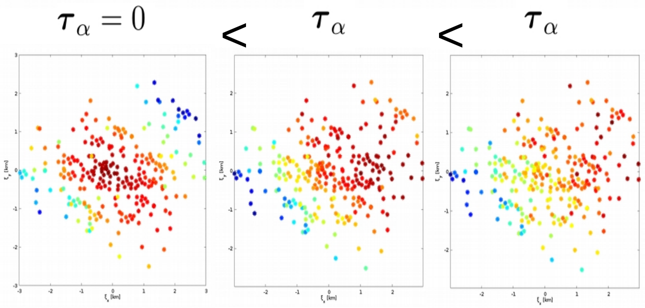

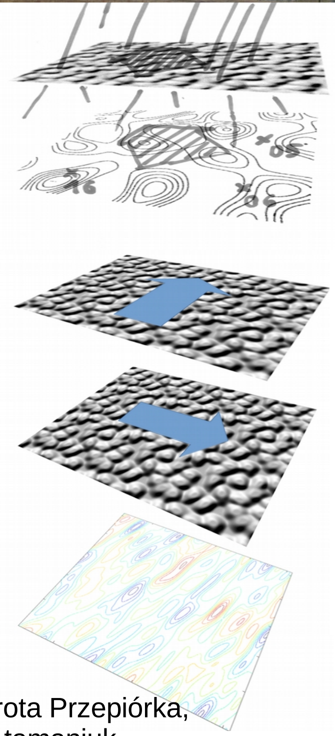

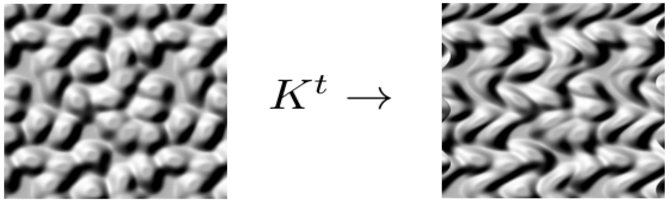

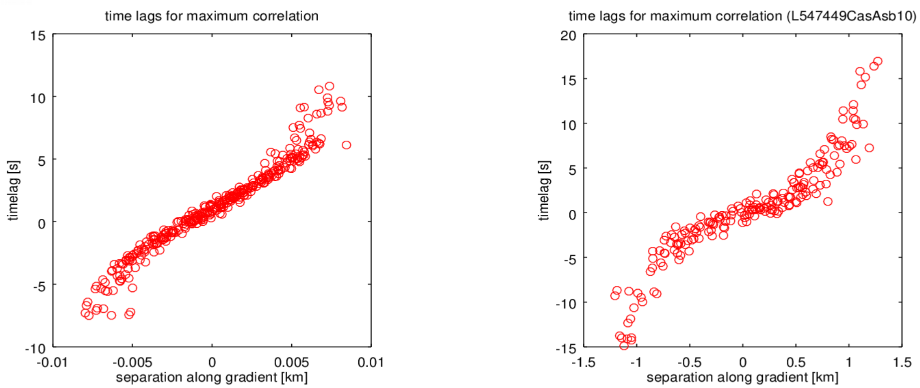

M. Grzesiak, Mariusz Pożoga, Barbara Matyjasiak, Dorota Przepiórka,
Hanna Rothkaehl, Katarzyna Budzińska, and Barbara Atamaniuk

EGU General Assembly 2021, online, 19–30 Apr 2021,
EGU21-6582, https://doi.org/10.5194/egusphere-egu21-6582, 2021.

LOFAR (Low Frequency Array)

Interferometry in low frequencies (10-240 MHz)

Consists of:

- Two antenna fields with 96 dipole antennas in each
- LBA (Low Band Antenna) – observations in 10-90 MHz range
- HBA (High Band Antenna) – observations in 110-240 MHz range
- Directional observations possible (beamforming)

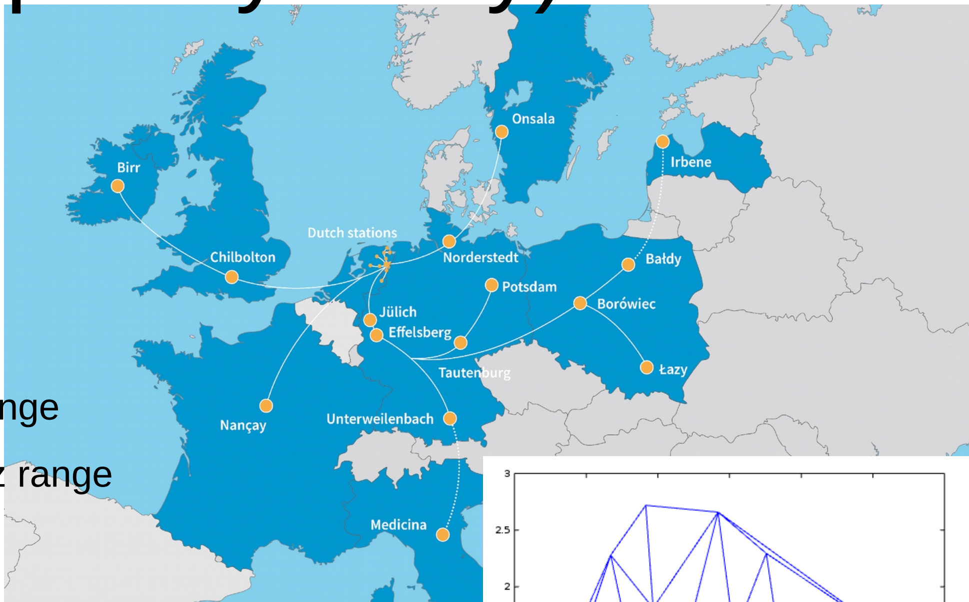

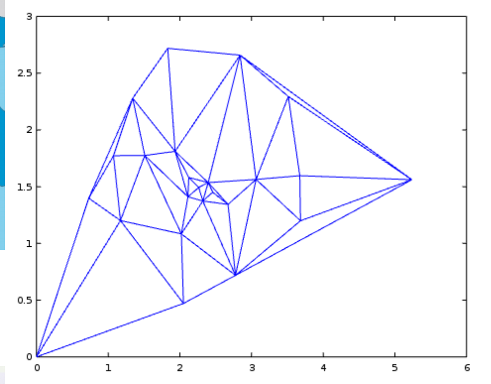

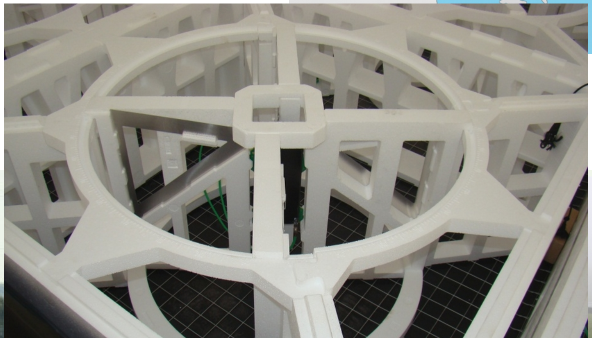

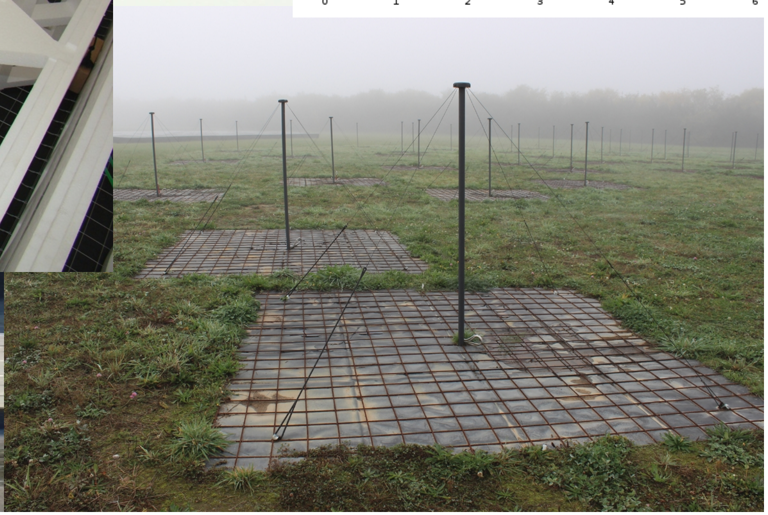

Scintillation

(fluctuations of wave characteristics after passing through medium with variable refractive index)

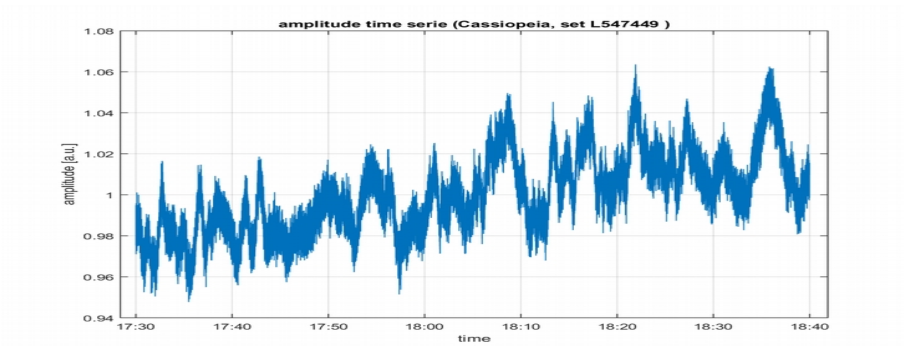

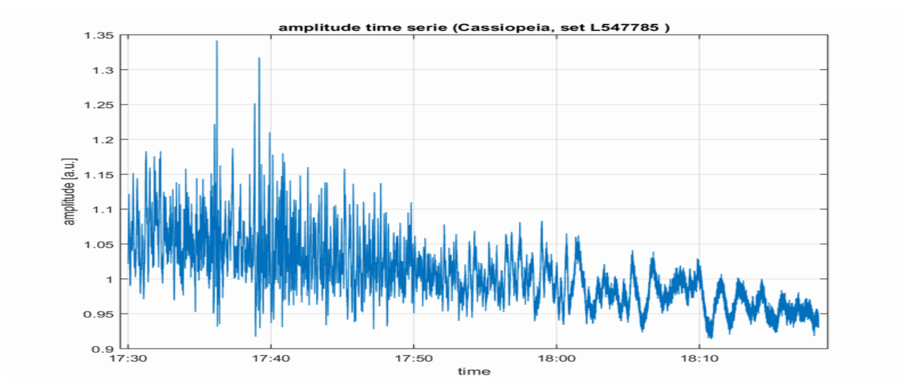

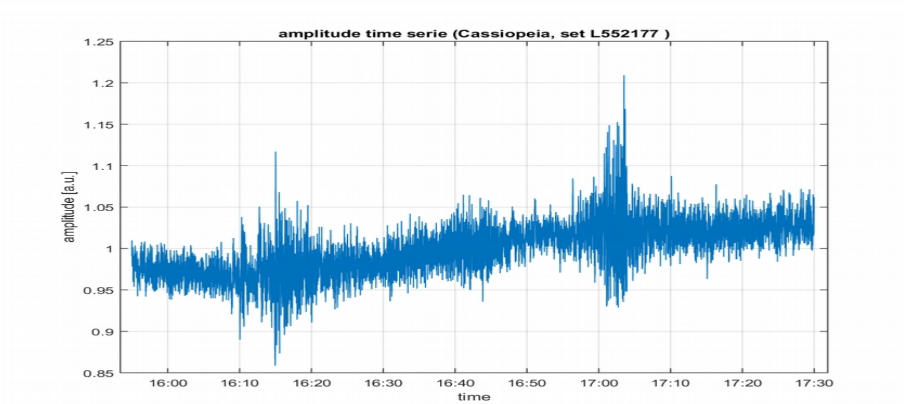

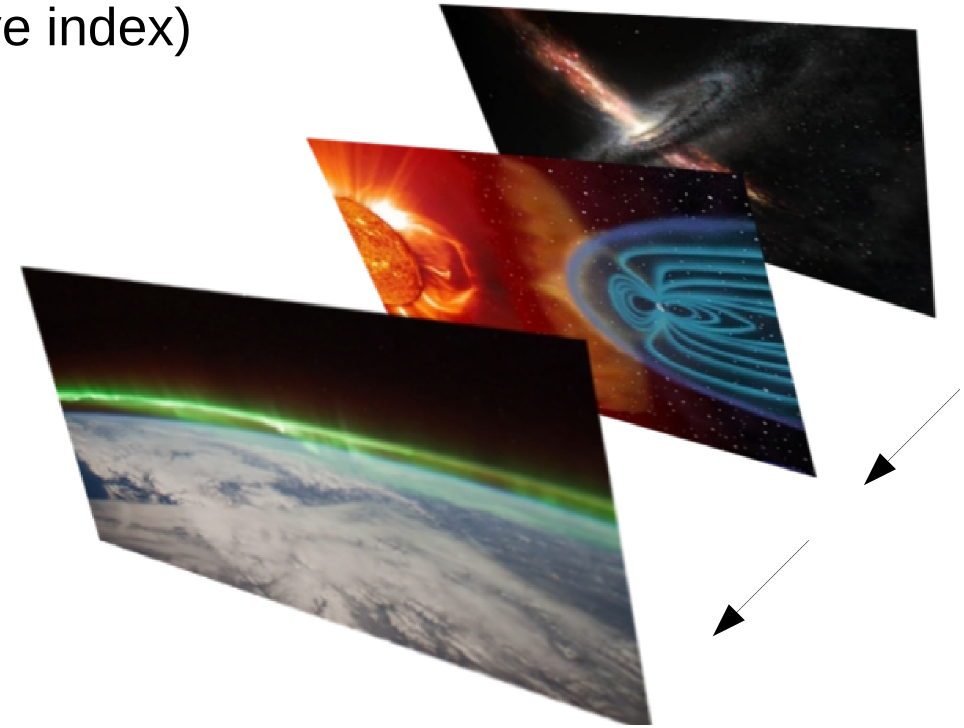

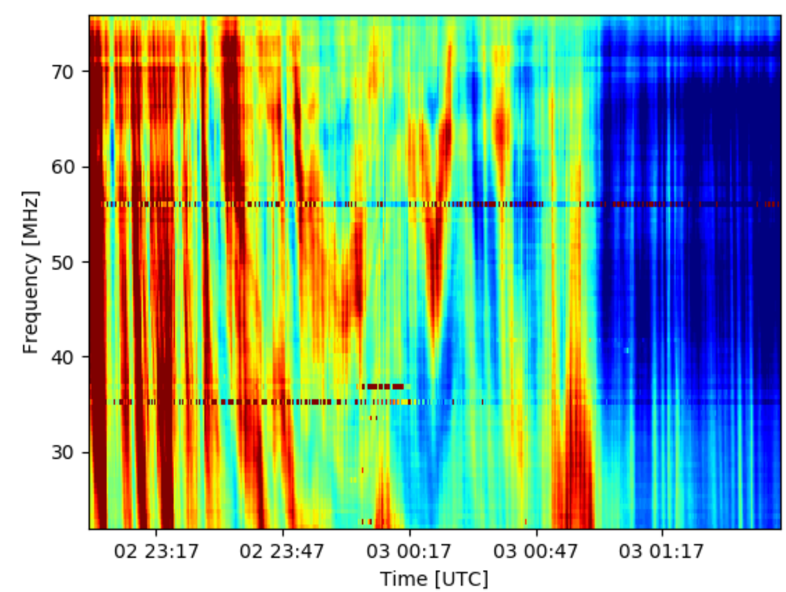

Modeling pattern evolution – dispersion analysis

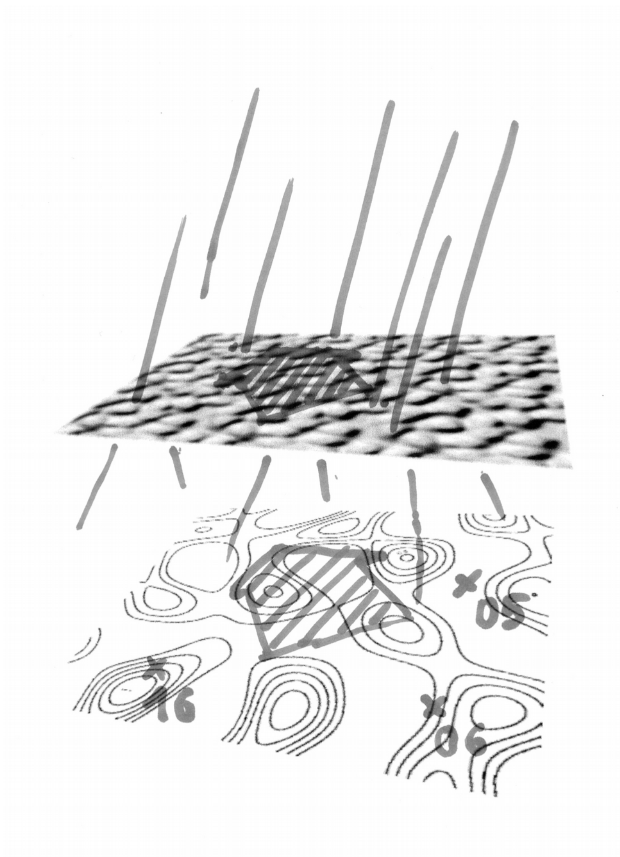

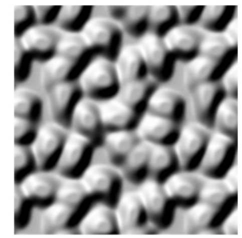 $K^t \rightarrow$ 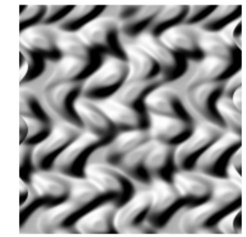

$$\psi(\mathbf{r},t) = \int d\mathbf{r}' K^t(\mathbf{r}-\mathbf{r}')\psi(\mathbf{r}',0)$$

$$\hat{\psi}(\mathbf{k},t) = \hat{\psi}(\mathbf{k},0)e^{\Omega(\mathbf{k})t}$$

$$\mathbb{E}[\psi(\boldsymbol{r}_1,t_1)\psi(\boldsymbol{r}_2,t_2)] = \int d\boldsymbol{k}P(\boldsymbol{k})e^{\Omega(\boldsymbol{k})\tau}e^{i\boldsymbol{k}\cdot\boldsymbol{\zeta}} = C(\boldsymbol{\zeta},\tau),$$

$$\boldsymbol{\zeta} = \boldsymbol{r}_2 - \boldsymbol{r}_1,\ \tau = t_2 - t_1$$

$$P(\boldsymbol{\zeta},\omega) = \int d\tau C(\boldsymbol{\zeta},\tau)e^{i\omega\tau} = \int d\tau e^{-i\omega\tau}\int d\boldsymbol{k}P(\boldsymbol{k})e^{\Omega(\boldsymbol{k})\tau}e^{i\boldsymbol{k}\cdot\boldsymbol{\zeta}} = \int d\boldsymbol{k}P(\boldsymbol{k})e^{i\boldsymbol{k}\cdot\boldsymbol{\zeta}}\delta(\omega-\Omega(\boldsymbol{k}))$$

$$<\boldsymbol{\zeta}> = \frac{\int d\boldsymbol{\zeta}\boldsymbol{\zeta}C(\boldsymbol{\zeta},\tau)}{\int d\boldsymbol{\zeta}C(\boldsymbol{\zeta},\tau)} \qquad \frac{\partial}{\partial\tau} <\boldsymbol{\zeta}> = \nabla_{\boldsymbol{k}}\Omega(\boldsymbol{k})|_{\boldsymbol{k}=0}$$

M. Grzesiak, A. W. Wernik, Dispersion analysis of spaced antenna measurements, Annales Geophysicae, 27, 2843-2849, 2009

Basic example – frozen flow

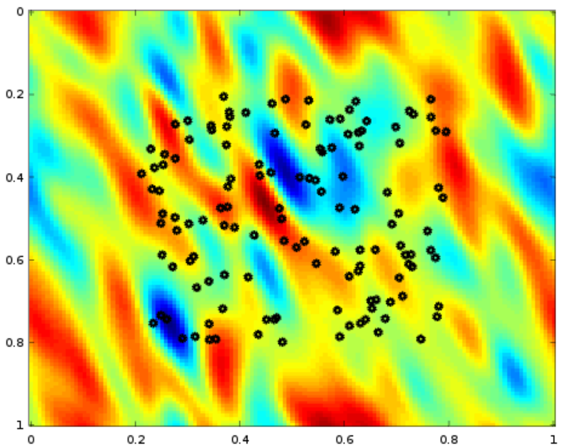

$$K(r' - r, t) = \delta(r' - (r - v_d t))$$

$$\frac{\partial}{\partial t} C - \mathbf{v} \cdot \nabla_{\boldsymbol{\xi}} C = 0$$

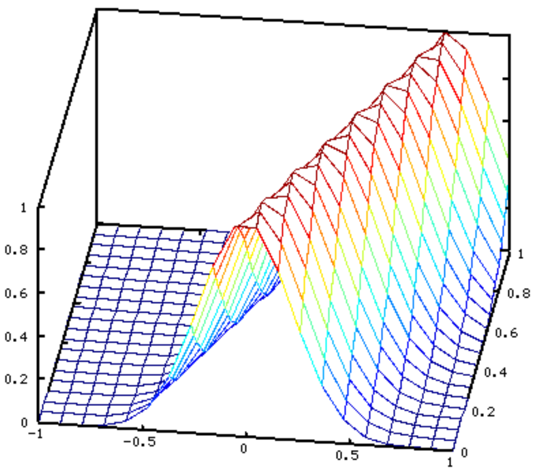

$$\boldsymbol{\xi}_\alpha = \mathbf{r}_k - \mathbf{r}_l$$

Simulation

Example from LOFAR

$\boldsymbol{\tau}_\alpha = 0$ < $\boldsymbol{\tau}_\alpha$

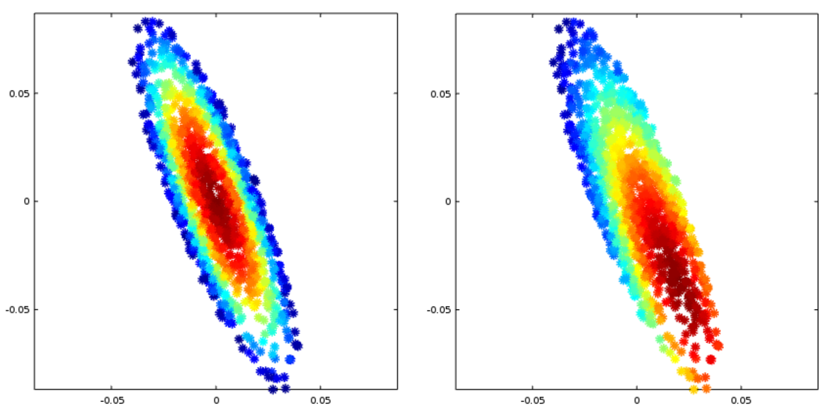

$\boldsymbol{\tau}_\alpha = 0$ < $\boldsymbol{\tau}_\alpha$ < $\boldsymbol{\tau}_\alpha$

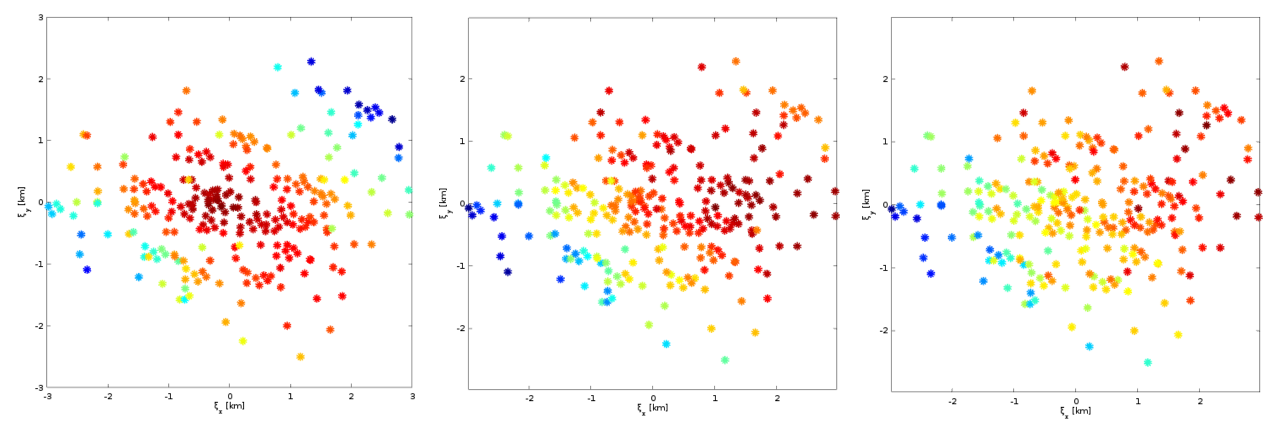

Correlation function features recognition

$$C(\boldsymbol{\xi} - \mathbf{v}\tau)$$

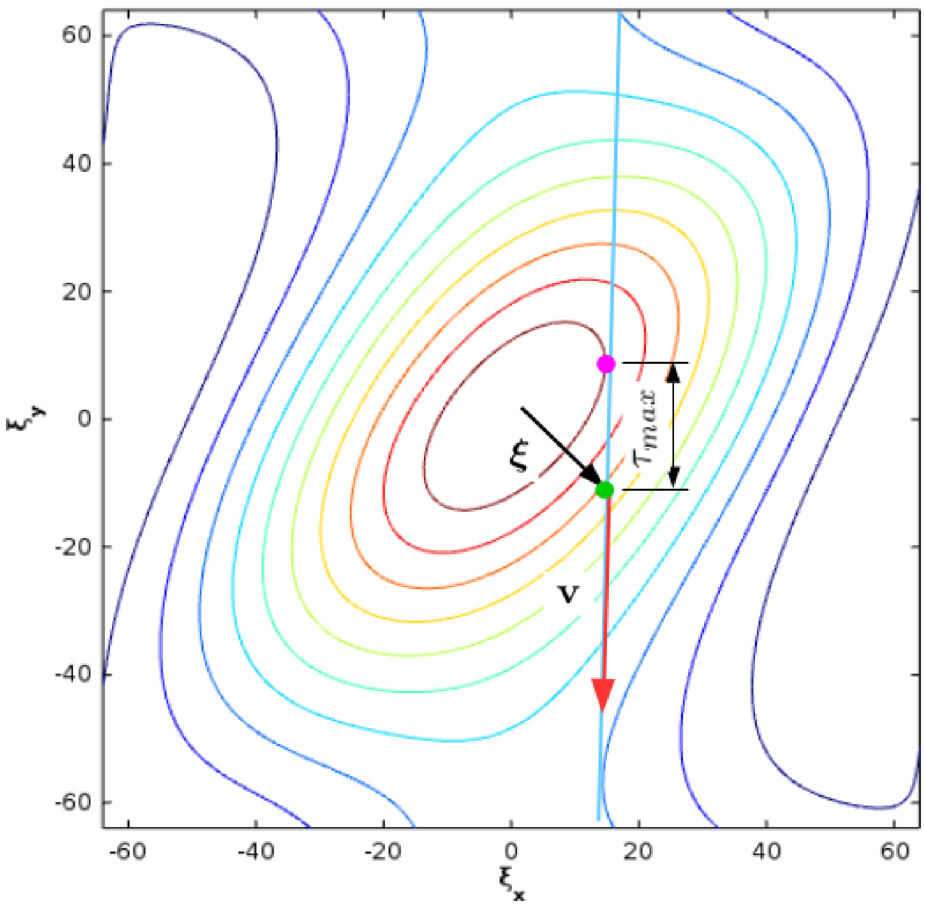

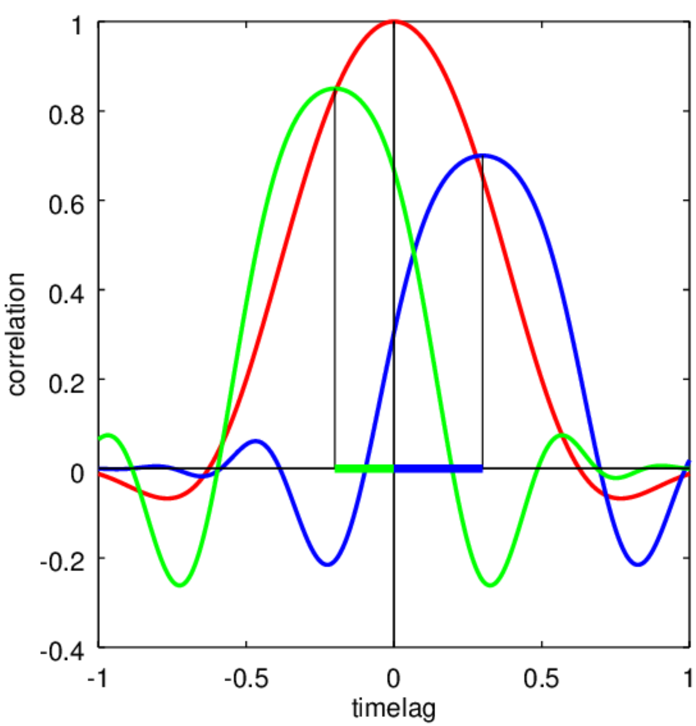

Briggs, B. H., On the analysis of moving patterns in geophysics,I, Correlation analysis, J. Atmos. Terr. Phys.,30, 1777-1788, 1968.

Estimation of geometry and drift velocity

$$C(\boldsymbol{\xi}) = \rho(\boldsymbol{\xi}^T Q \boldsymbol{\xi})$$

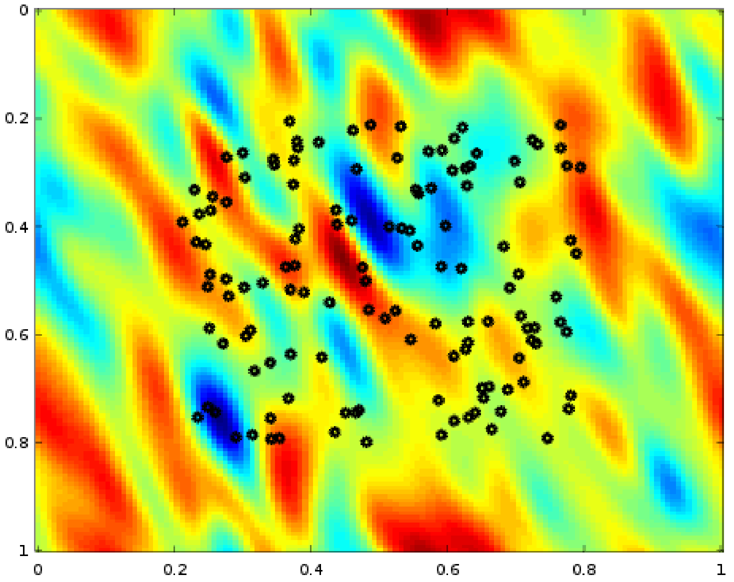

$$\frac{\partial}{\partial \tau} C(\boldsymbol{\xi} - \boldsymbol{v}\tau) = 0 \qquad \boldsymbol{\xi}^T Q \boldsymbol{v} = \tau_m \boldsymbol{v}^T Q \boldsymbol{v} \rightarrow \tau_m = \frac{\boldsymbol{\xi}^T Q \boldsymbol{v}}{\boldsymbol{v}^T Q \boldsymbol{v}}$$

$$\nabla_\xi \tau_m = \frac{Q\boldsymbol{v}}{\boldsymbol{v}^T Q \boldsymbol{v}} \qquad \boldsymbol{v} = \frac{Q^{-1} \nabla_\xi \tau_m}{(\nabla_\xi \tau_m)^T Q^{-1} \nabla_\xi \tau_m}$$

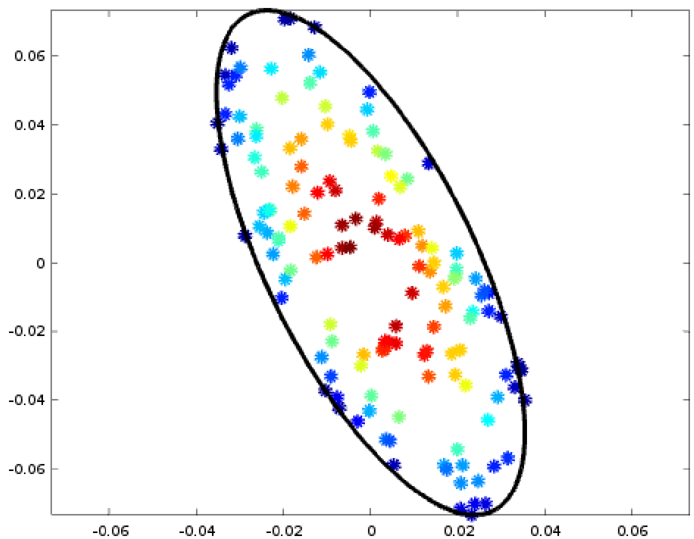

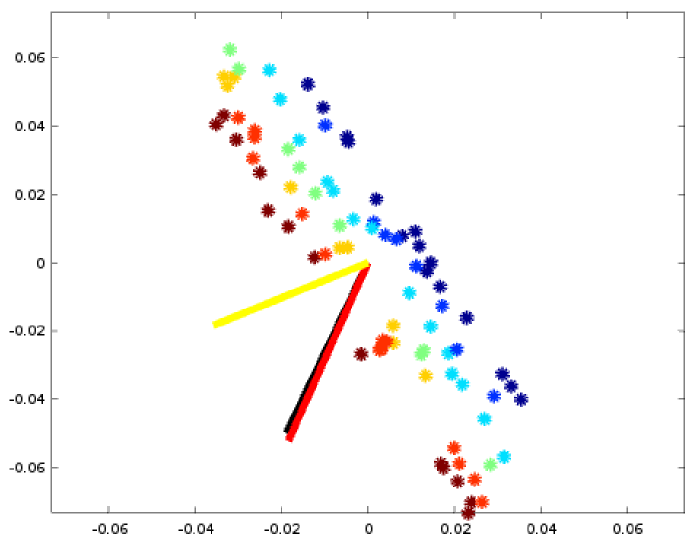

Estimation of geometry and drift velocity

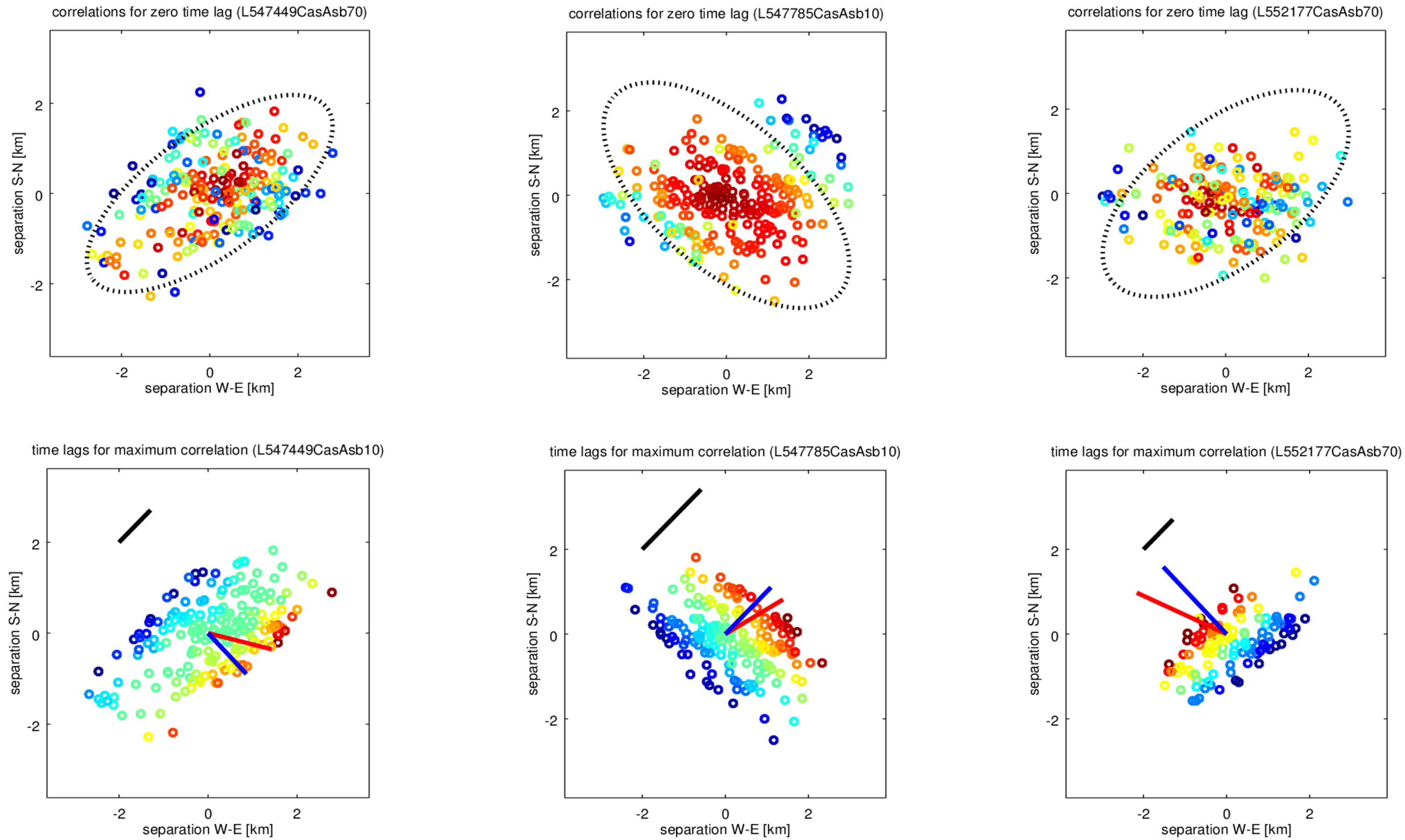

data set	v_x [m/s]	v_y [m/s]	magnitude [m/s]	v_x isotropic [m/s]	v_y isotropic [m/s]	magnitude isotropic [m/s]
L547449	142	-35	147	86	-90	124
L547785	694	408	804	549	552	778
L552177	-2160	795	2370	-1526	1586	2200

Space-frequency analysis

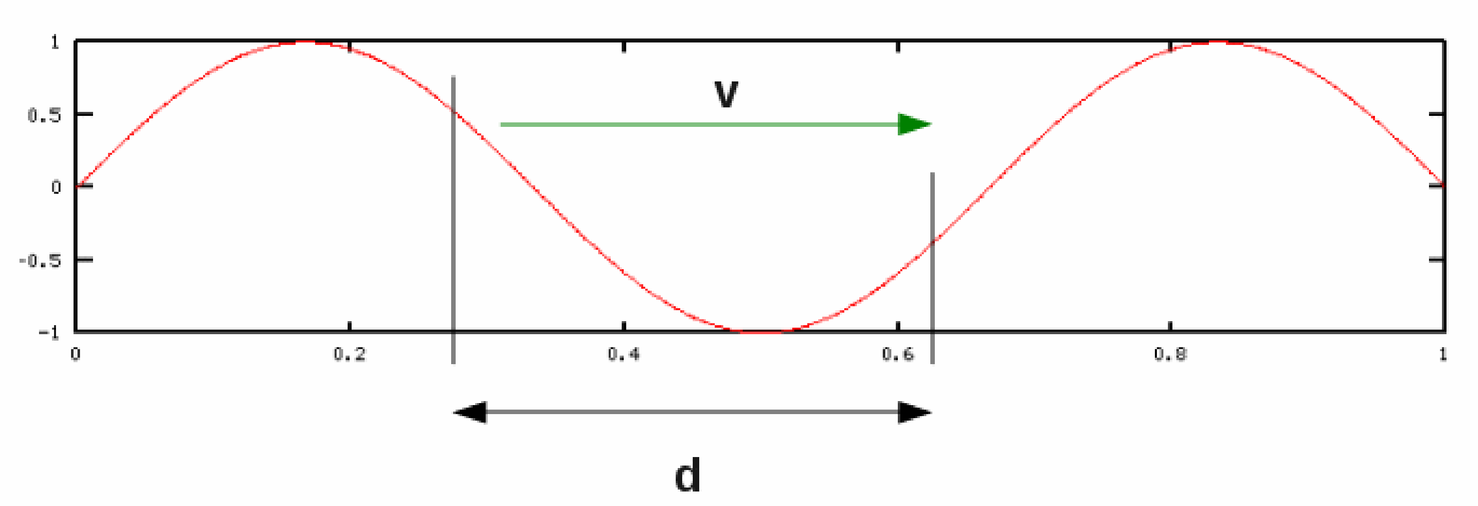

$$f = \exp ikx \qquad x \to x - vt$$

$$f(x_1, t_1) f^*(x_2, t_2) = \exp(ikd) exp(ikv\tau),\ d = x_1 - x_2,\ \tau = t_1 - t_2$$

$$\omega = kv,\ \Delta\phi = kd \to \Delta\phi = \frac{d}{v}\omega$$

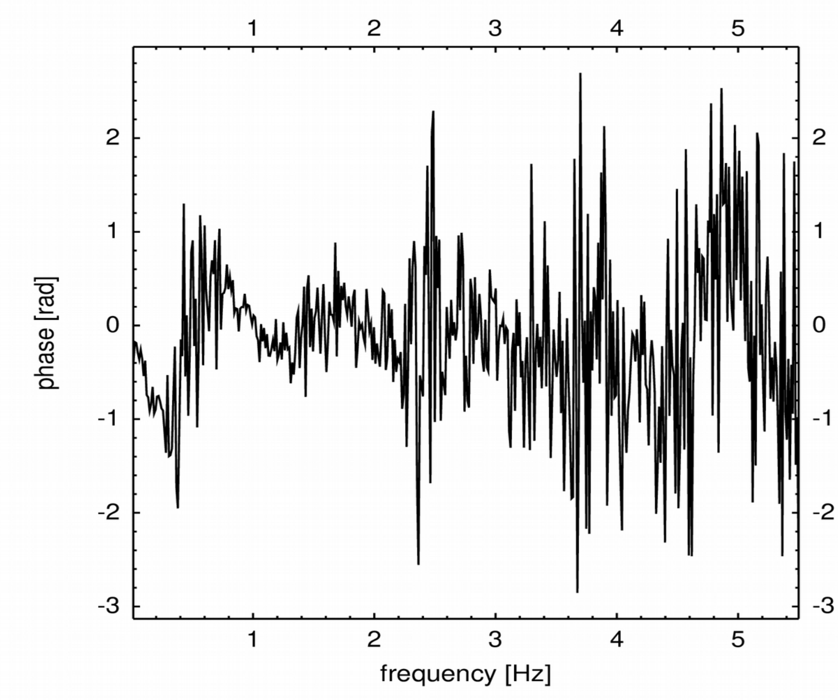

Frequency domain picture

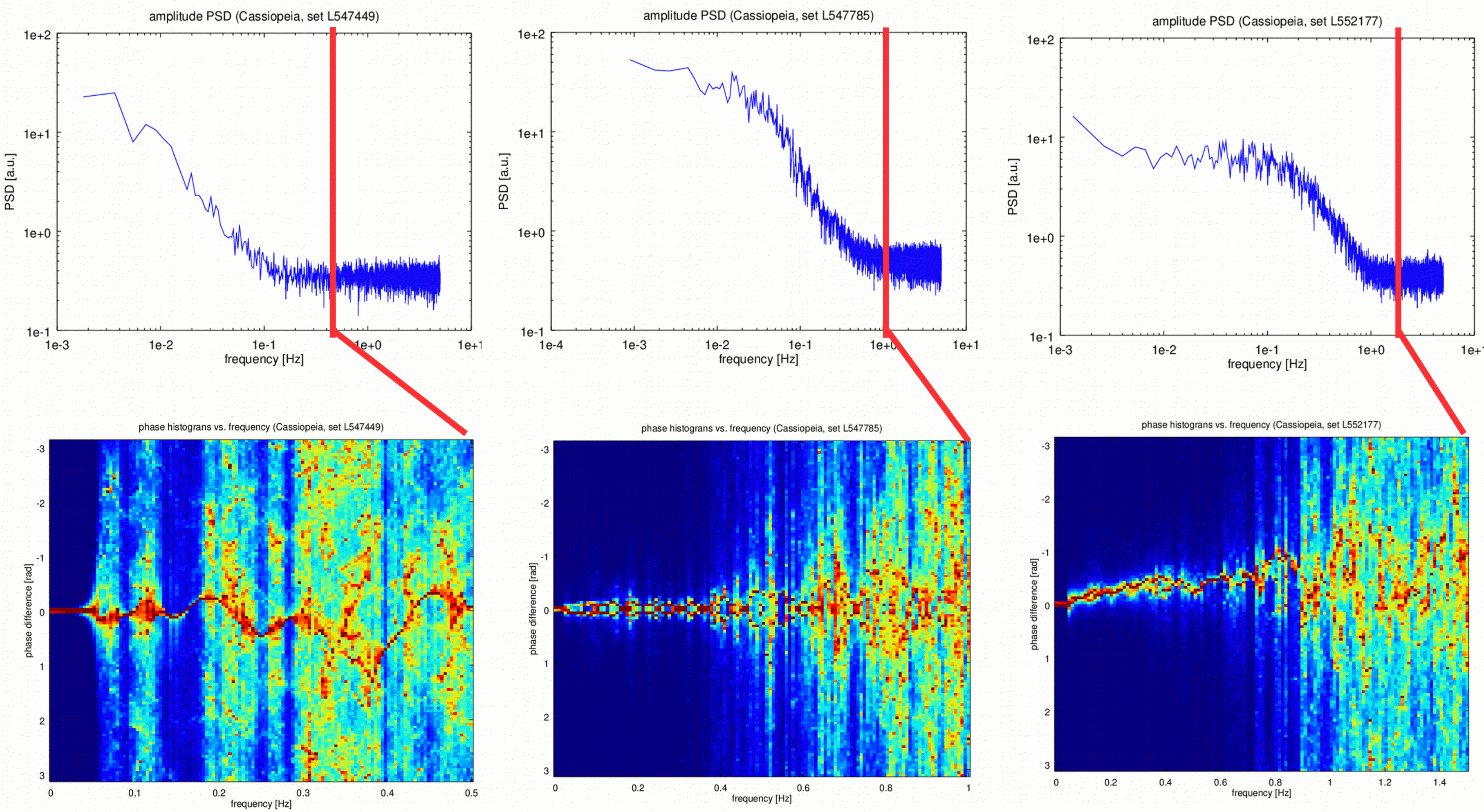

Time vs. frequency

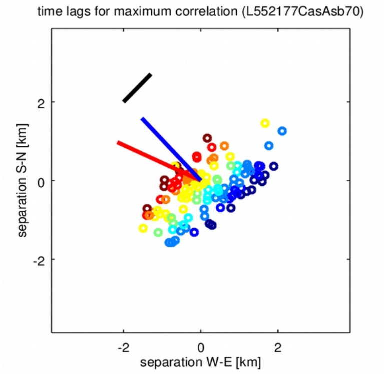

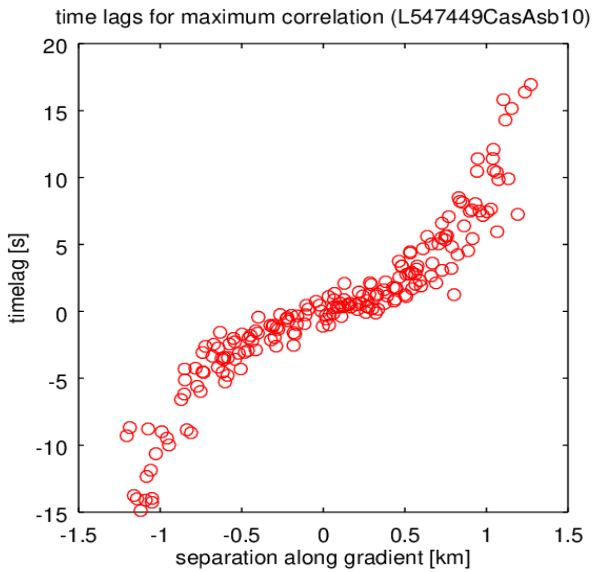

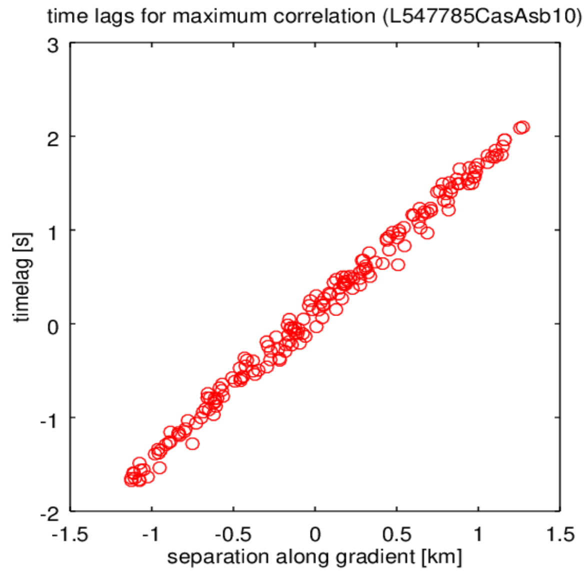

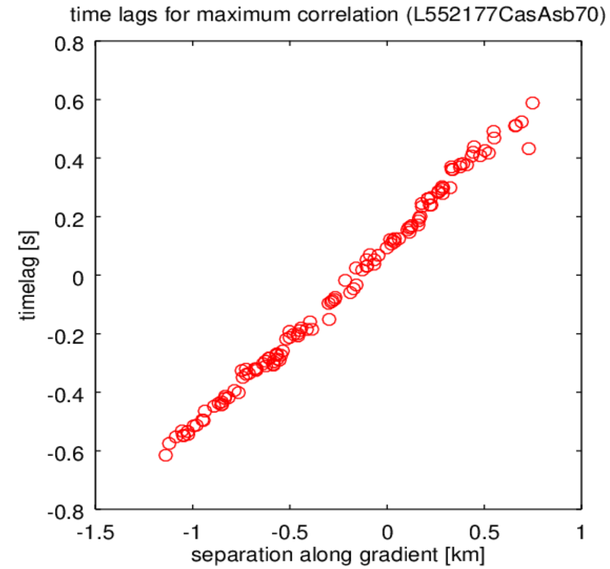

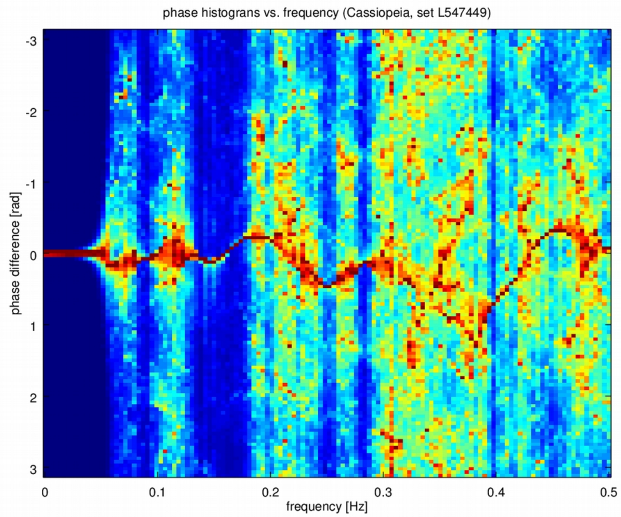

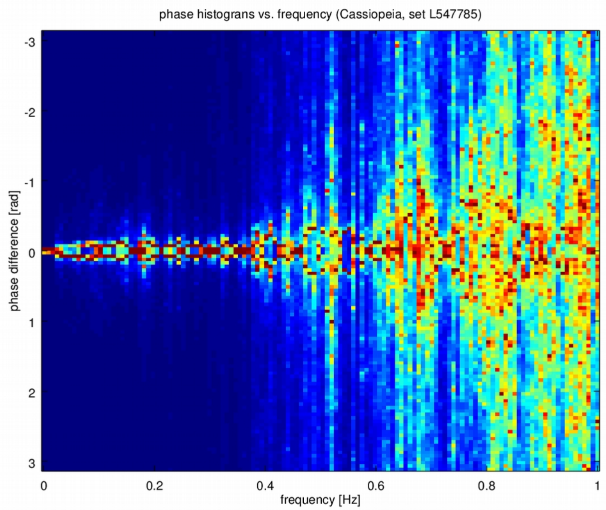

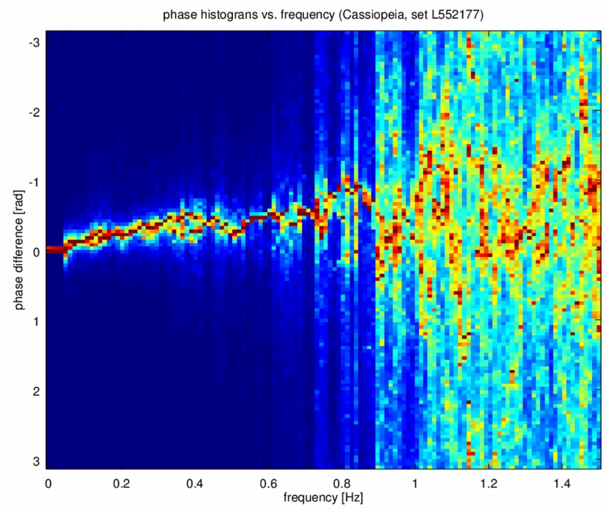

Phase screen approach & Fresnel filtering

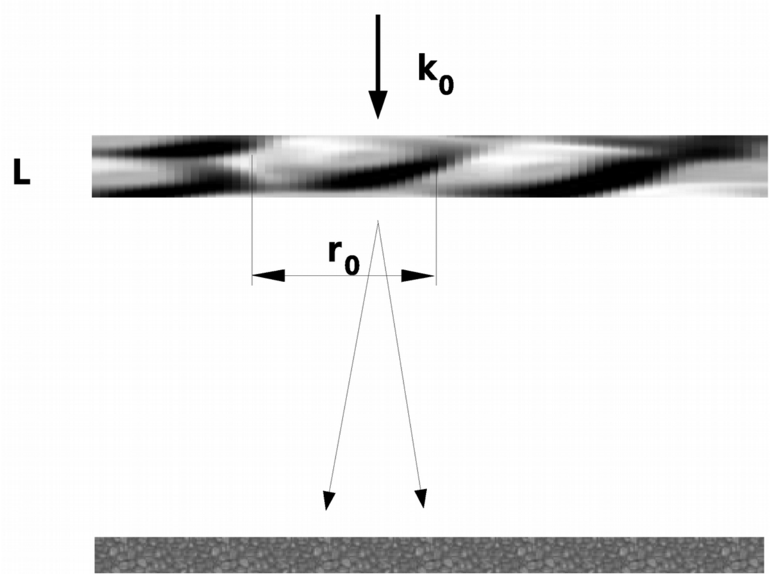

$$\sqrt{\lambda L} \ll r_0$$

$$u(\mathbf{r}_\perp, z) = u_0 \frac{ik_0}{2\pi z} \int d\mathbf{r}'_\perp \exp\left[-i\left(\frac{k_0(\mathbf{r}_\perp - \mathbf{r}'_\perp)^2}{2z} + \delta\phi(\mathbf{r}'_\perp)\right)\right]$$

$$\delta\phi(\mathbf{r}_\perp) = -r_e \lambda \int dl \Delta N_e(\mathbf{r}_\perp, l)$$

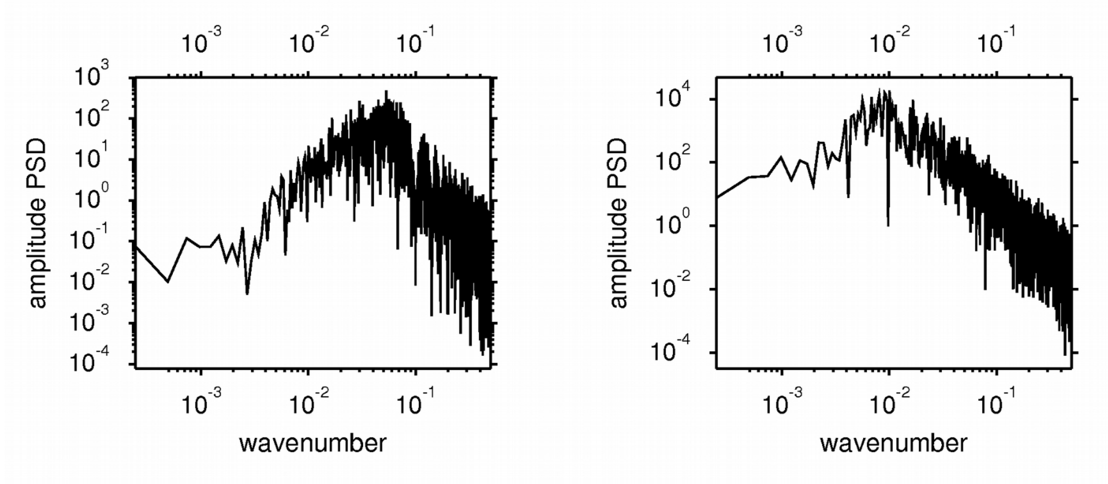

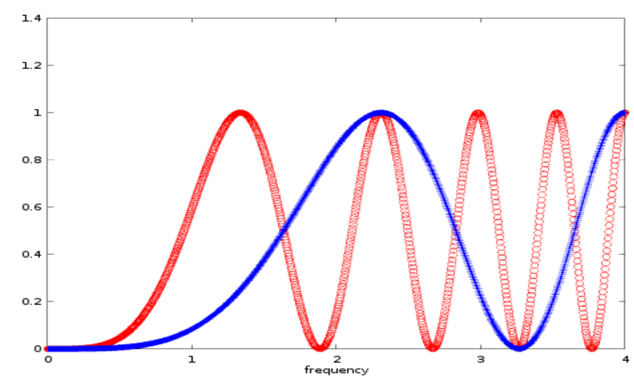

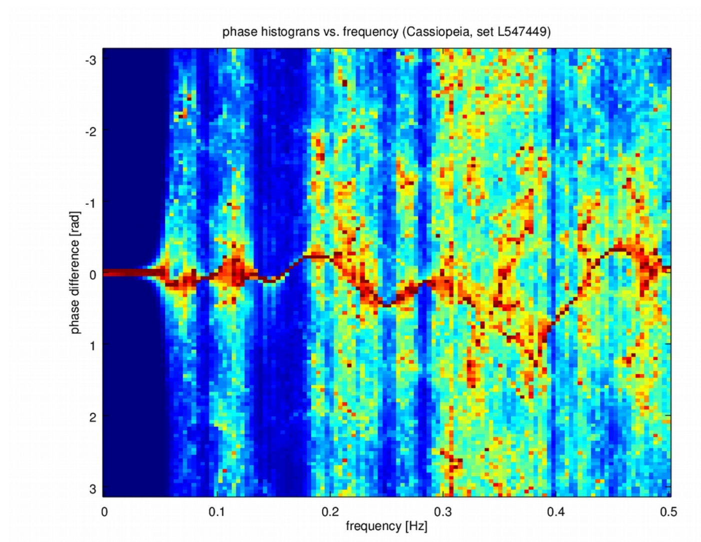

Double phase screen

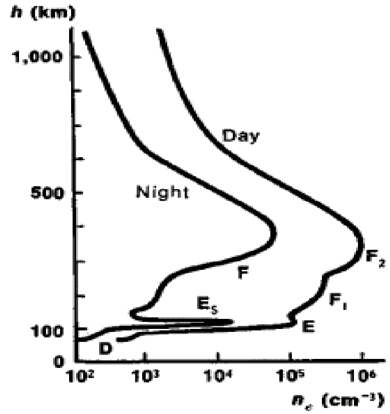

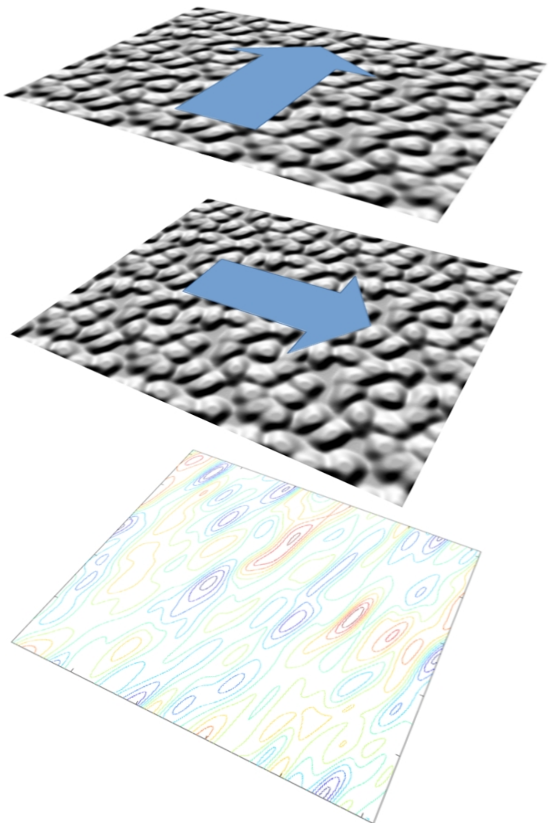

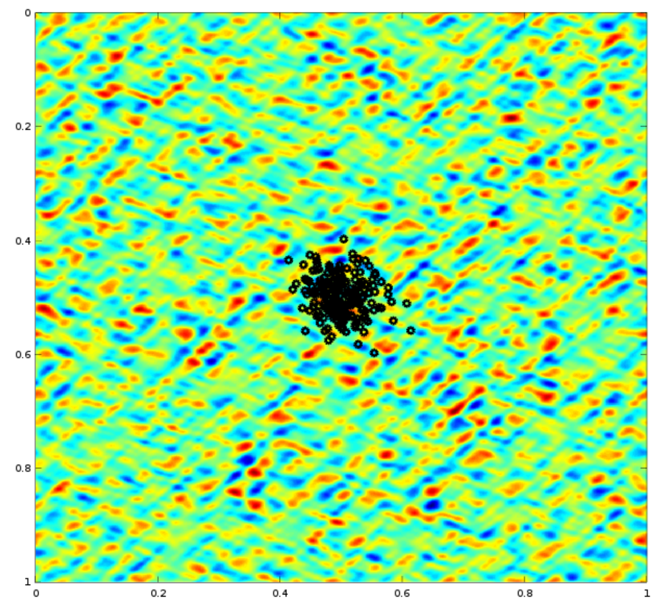

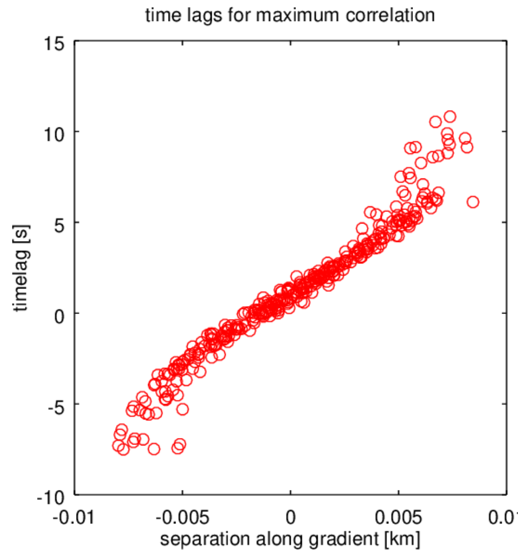

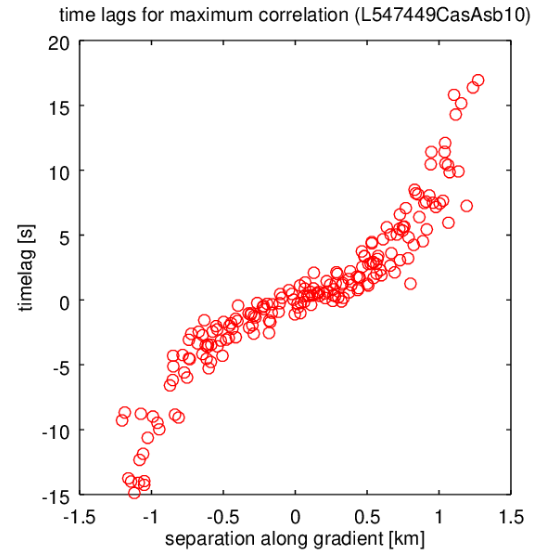

Problems with frozen flow model

Velocity rescaled

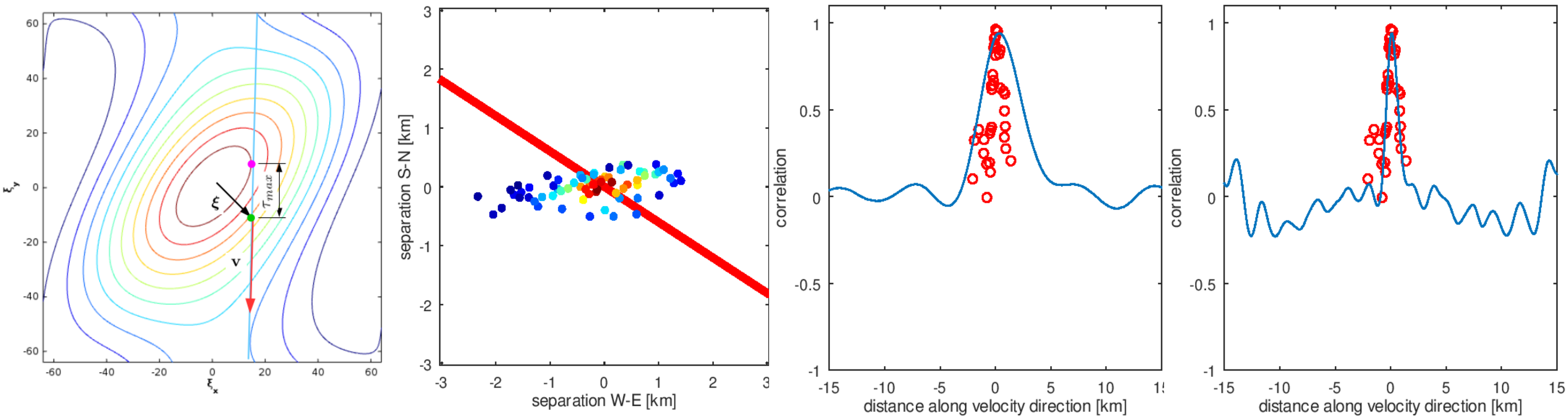

Temporal decorrelation + frozen flow: $Q' = T^T Q T$

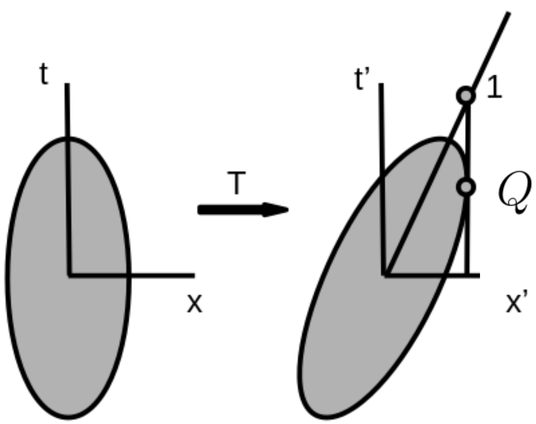

$$Q = \begin{bmatrix} Q_s & 0 \\ 0 & \beta \end{bmatrix}, T = \begin{bmatrix} 1 & 0 & v_x \\ 0 & 1 & v_y \\ 0 & 0 & 1 \end{bmatrix} = \begin{bmatrix} I & \mathbf{v} \\ \mathbf{0}^T & 1 \end{bmatrix}, Q' = \begin{bmatrix} Q_s & Q_s\mathbf{v} \\ \mathbf{v}^T Q_s & \beta + \mathbf{v}^T Q_s \mathbf{v} \end{bmatrix}$$

$$\mathbf{v}_T = Q_s^{-1} Q_{[1:2;3]}$$

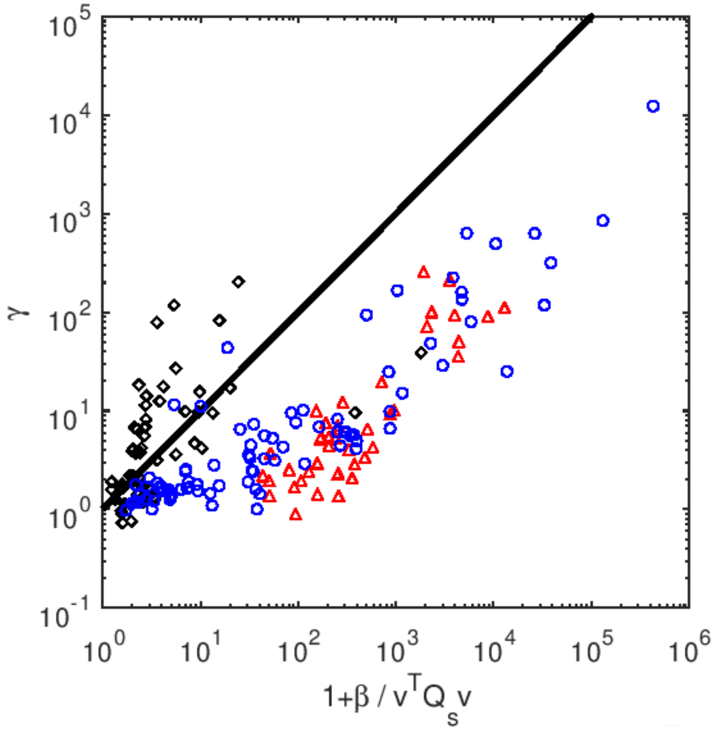

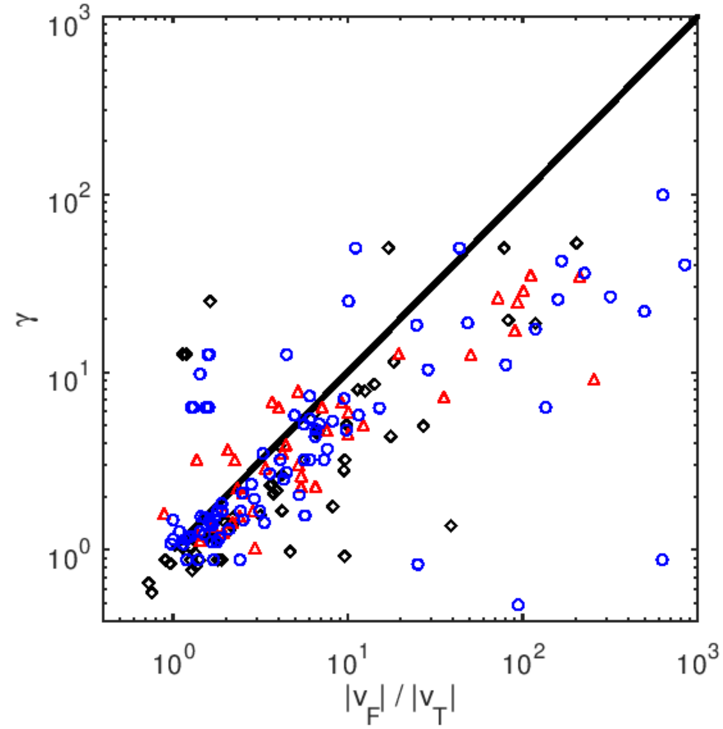

$$\mathbf{v}_F = (1 + \beta / \mathbf{v}_T^T Q_s \mathbf{v}_T)\mathbf{v}_T$$

γ – the velocity scaling factor from fitting the temporal correlation to the spatial correlation

v_F – the velocity when taken the frozen flow approximation

Estimated velocity doesn’t follow model with separable temporal decorrelation

Conclusions

LOFAR network provides consistent scintillation data of coverage both in time and space that equips us with new possibilities of Spatio-temporal analysis.

The method presented gives an estimate of drift velocity, taking into account possible anisotropy of irregularities. It turns out that the magnitude of drift velocity depends on geomagnetic activity: the larger the Kp index, the greater velocity, which is in agreement with previous observations.

Similar scales of irregularities revealed by correlation analysis at a given time instant in conjunction with velocity estimates explain the broadening of frequency power spectra - larger drift velocity shifts spatial structures in the frequency domain according to the Doppler effect.

The observed nonlinear dependence of time lag on separation can be attributed to propagation through a multilayer ionosphere with different evolution properties.

There are inconsistencies between the observations and the frozen flow model that cannot be accounted for by the temporal decorrelation.